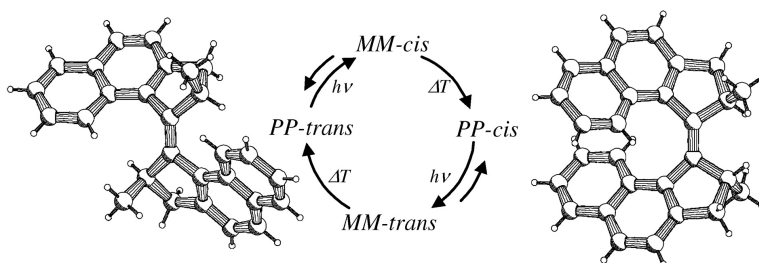Article

Increased Speed of Rotation for the Smallest Light-Driven Molecular Motor

Matthijs K. J. ter Wiel, Richard A. van Delden, Auke Meetsma, and Ben L. Feringa

More About This Article

Additional resources and features associated with this article are available within the HTML version:

- Supporting Information
- Access to high resolution figures
- Links to articles and content related to this article
- Copyright permission to reproduce figures and/or text from this article

View the Full Text HTML

Increased Speed of Rotation for the Smallest Light-Driven Molecular Motor

Matthijs K. J. ter Wiel, Richard A. van Delden, Auke Meetsma, and Ben L. Feringa*

Contribution from the Department of Organic Chemistry, Stratingh Institute, University of Groningen, Nijenborgh 4, 9747 AG, Groningen, The Netherlands

Received June 19, 2003; E-mail: feringa@chem.rug.nl

Abstract: In this paper we present the smallest artificial light-driven molecular motor consisting of only 28 carbon and 24 hydrogen atoms. The concept of controlling directionality of rotary movement at the molecular level by introduction of a stereogenic center next to the central olefinic bond of a sterically overcrowded alkene does not only hold for molecular motors with six-membered rings, but is also applicable to achieve the unidirectional movement for molecular motors having five-membered rings. Although X-ray analyses show that the five-membered rings in the *cis*- and *trans*-isomer of the new molecular motor are nearly flat, the energy differences between the (pseudo-)diaxial and (pseudo-)diequatorial conformations of the methyl substituents in both isomers are still large enough to direct the rotation of one-half of the molecule with respect to the other half in a clockwise fashion. The full rotary cycle comprises four consecutive steps: two photochemical isomerizations each followed by a thermal helix inversion. Both photochemical *cis–trans* isomerizations proceed with a preference for the unstable diequatorial isomers over the stable diaxial isomers. The thermal barriers for helix inversion of this motor molecule have decreased dramatically compared to its six-membered ring analogue, the half-life of the fastest step being only 18 s at room temperature.

Introduction

The bottom-up construction of molecular-level machines is one of the most challenging tasks in the pursuit of nanotechnology.[1] Nature's molecular machinery such as the ATP synthase,[2] kinesine and myosine,[3] and flagellar motors in bacteria serve as a major source of inspiration for the development of artificial molecular devices such as molecular switches,[4] motors,[5,6] shuttles,[7] scissors,[8] rotating modules,[9] and muscles.[10]

A sophisticated synthetic system that mimics the behavior of naturally occurring processive enzymes has recently been reported by Nolte et al.[11] Emphasis is currently shifting to multifunctional or organized molecules and systems that can perform a certain task, for instance, by mounting them on a surface[12] or inclusion in a liquid crystalline matrix.[13] An especially elegant example is the molecular machine by Gaub et al.,[14] featuring a polymer consisting of azobenzenes which is stretched and contracted on application of external stimuli and thus is able to perform work. A vital component of the nanotechnology toolbox would be a molecule or molecular assembly that acts as a motor, driving (mechanical) processes at the molecular level. The design of such a device has to fulfill a number of requirements. The motor molecule has to escape from the Brownian motion; its movement has to be controlled and needs to be unidirectional.[5] Second, the molecule has to be able to perform the same cycle of movements a large number of times to function as a motor. Finally, the motor molecule has to perform work and should therefore be able to convert one type of energy into another. Only a few systems have proven to stand the challenge made by these demands.[15]

(1) *Sci. Am. Special Issue: Nanotech: The Science of Small Gets Down to Business*, Sept **2001**. (b) Feynman, R. P. In *Miniturization*; Gilbert H. D., Ed.; Reinhold, New York; 1961. (c) Drexler, K. E. *Nanosystems: Molecular Machinery, Manufacturing and Computation*; Wiley: New York, 1992. (d) Astumian, R. D. *Sci. Am.* **2001**, *285* (1), 56–64.
(2) Yin, H.; Wang, M. D.; Svoboda, K.; Landick, R.; Block, S. M.; Gelles, J. *Science* **1995**, *270*, 1653–1657. (b) Walker, J. E. *Angew. Chem., Int. Ed. Engl.* **1998**, *37*, 2309–2319. (c) Boyer, P. D. *Angew. Chem., Int. Ed. Engl.* **1998**, *37*, 2297–2307.
(3) Vale, R. D.; Milligan, R. A. *Science* **2000**, *288*, 88–95 and references therein.
(4) (a) Feringa, B. L.; van Delden, R. A.; ter Wiel, M. K. J. In *Molecular Switches*; Feringa, B. L., Ed.; Wiley-VCH: Weinheim, 2001; Chapter 5, pp 123–163. (b) Feringa, B. L.; van Delden, R. A.; Koumura, N.; Geertsema, E. M. *Chem. Rev.* **2000**, *100*, 1789–1816.
(5) (a) Feringa, B. L. *Acc. Chem. Res.* **2001**, *34*, 504–513. (b) Kelly, T. R. *Acc. Chem. Res.* **2001**, *34*, 514–522. (b) Kelly, T. R.; De Silva, H.; Silva, R. A. *Nature* **1999**, *401*, 150–152.
(6) (a) Balzani, V.; Credi, A.; Raymo, F. M.; Stoddart, J. F. *Angew. Chem., Int. Ed.* **2000**, *39*, 3349–3391. (b) Leigh, D. A.; Wong, J. K. Y.; Dehez, F.; Zerbetto, F. *Nature* **2003**, *424*, 174–179.
(7) (a) Ballardini, R.; Balzani, V.; Credi, A.; Gandolfi, M. T.; Venturi, M. *Acc. Chem. Res.* **2001**, *34*, 445–455. (b) Pease, A. R.; Jeppesen, J. O.; Stoddart, J. F.; Luo, Y.; Collier, C. P.; Heath, J. R. *Acc. Chem. Res.* **2001**, *34*, 433–444. (c) Brouwer, A. M.; Frochot, C.; Gatti, F. G.; Leigh, D. A.; Mottier, L.; Paolucci, F.; Roffia, S.; Wurpel, G. W. H. *Science* **2001**, *291*, 2124–2128.
(8) Muraoka, T.; Kinbara, K.; Kobayashi, Y.; Aida, T. *J. Am. Chem. Soc.* **2003**, *125*, 5612–5613.
(9) Tashiro, K.; Konishi, K.; Aida, T. *J. Am. Chem. Soc.* **2000**, *122*, 7921–7926.
(10) Jiménez, M. C.; Dietrich-Buchecker, C.; Sauvage, J.-P. *Angew. Chem., Int. Ed.* **2000**, *39*, 3284–3287.
(11) Thordarson, P.; Bijsterveld, E. J. A.; Rowan, A. E.; Nolte, R. J. M. *Nature* **2003**, *424*, 915–918.
(12) Chia, S. Y.; Cao, J. G.; Stoddart, J. F.; Zink, J. I. *Angew. Chem., Int. Ed.* **2001**, *40*, 2447–2451.
(13) van Delden, R. A.; Koumura, N.; Harada, H.; Feringa, B. L. *Proc. Nat. Acad. Sci.* **2002**, *99*, 4945–4949.
(14) Hugel, T.; Holland, N. B.; Cattani, A.; Moroder, L.; Seitz, M.; Gaub, H. E. *Science* **2002**, *296*, 1103–1106.
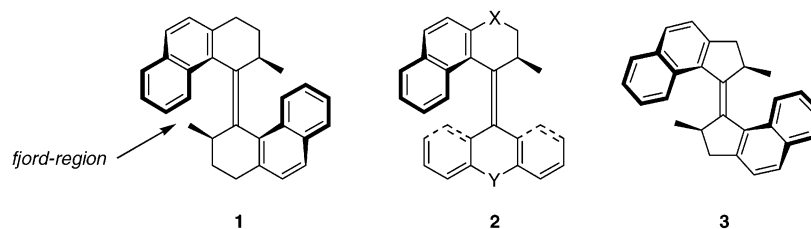
Figure 1. First- and second-generation light-driven molecular motors **1** and **2** and the new motor **3**.

Our design of nanomechanical motors has focused on the light-driven unidirectional rotary movement found in symmetrical overcrowded biphenanthrylidene **1** (Figure 1).[16] This was the first system capable of performing a unidirectional 360° rotation, with one-half of the molecule rotating with respect to the other half of the molecule. Key features of this motor are the intrinsic helical shape, the photoisomerizable carbon–carbon double bond that acts as the axis of rotation, and two stereogenic centers, each in one-half of the molecule. The unidirectional rotary motion of this system involves four consecutive steps: two energetically uphill photochemical steps each followed by an energetically downhill thermal step. In this process, fueled by light energy, unidirectionality is achieved by the subtle interplay between the conformation of the six-membered ring and the orientations which the methyl substituents can adopt. Due to the steric hindrance in these molecules, the (pseudo-)axial orientation is energetically preferred over the (pseudo-)equatorial orientation of the methyl substituent in both the *cis*- and *trans*-isomer of **1**.

Upon irradiation, *trans*–*cis* isomerization occurs and the overall helicity of the molecule is inverted. Simultaneously, due to a change in conformation of the six-membered ring, the methyl substituents are forced to adopt a disfavored (pseudo-)equatorial orientation. Heating of the molecules in their less stable conformations results in an inversion of helicity and the methyl substituents adopt a favored (pseudo-)axial orientation again. When doped in a liquid crystalline matrix, motor molecule **1** was able to drive a color change amplifying motion at the molecular level to a macroscopically observable effect.[13] However, this first-generation molecular motor still has a substantial number of properties that need improvement in order to further develop the concept of light-driven motors for future nanomechanical applications. A drawback of this prototype system is the high energy barrier to accomplish the thermally driven helix inversion, which is a crucial factor in the control of the speed of rotary motion. In one approach to overcome this shortcoming, the so-called second-generation molecular motor **2** was designed (Figure 1). These molecules consists of two entities: a rotor part with a single stereogenic center governing unidirectional rotation and a stator part where substituents can be introduced allowing functionalization to more elaborate motor systems.[17] It has been shown that changing the steric hindrance around the *fjord region* (Figure 1) can have a

large influence on the overall geometry of the molecule and therefore on the thermal helix inversion steps involved in the rotary motion. By adapting the size of the atoms (X,Y) in both the upper and lower parts of this molecule, the thermal barrier for helix inversion can be decreased substantially.[17b,18] From these studies it is evident that a subtle balance of structural parameters governs the rate of rotary motion. It appeared to us that the size and the geometry of the rings connecting upper and lower halves to the central carbon–carbon double bond in **1** might be an important factor in controlling the rotation speed. In the present paper a new motor molecule is presented, featuring five-membered instead of six-membered rings connected to the central olefinic bond, which results in a drastic enhancement of the speed of rotation.

Molecular Design

The rate-determining step for the 360° rotation around the double bond for all motor molecules investigated so far is the thermally driven helix inversion. Although improvements have been made in the lowering of the barrier for this conversion, the fastest molecular motor molecule still has a half-life of 2400 s for the thermal helix inversion at room temperature.[17b] The challenge is to further decrease these barriers without affecting the unidirectional rotation. Particularly important with respect to new and improved designs of molecular motors based on sterically overcrowded alkenes are the geometry and conformation around the central double bond and the steric hindrance around the *fjord region*. The molecular motors described so far always contained one or two six-membered rings with stereogenic centers controlling the direction of rotation. Since these six-membered rings introduce considerable steric hindrance into the molecule, a pertinent question is whether the presence of a smaller five-membered ring bearing a stereogenic center as in **3** (Figure 1) would allow a faster unidirectional 360° rotation.

Comparing the six- and five-membered ring systems **1** and **3**, a number of factors which are of importance for both the photochemical and thermal steps involved in the rotational process have to be considered. The larger six-membered rings in **1** will push the two naphthalene moieties in the upper and lower halves of the molecule stronger toward each other than would be the case for **3** containing five-membered rings. The second consideration is the orientation of the methyl substituent at the stereogenic center and the conformation of the ring to which it is attached. The highly distorted six-membered ring in **1**, which has a boatlike conformation, contains three sp^2-hybridized carbon atoms. The five-membered ring in **3** also contains three sp^2-hybridized carbon atoms and is therefore expected to be close to planarity. A key question is whether

(15) (a) Feringa, B. L.; Koumura, N.; van Delden, R. A. *Appl. Phys. A* **2002**, *75*, 301–308. (b) Feringa, B. L.; van Delden, R. A.; ter Wiel, M. K. J. *Pure Appl. Chem.* **2003**, *75*, 563–575.

(16) (a) Koumura, N.; Zijlstra, R. W. J.; van Delden, R. A.; Harada, N.; Feringa, B. L. *Nature* **1999**, *401*, 152–155. (b) For commentary on both the chemically and photochemically driven molecular motors, see: Davis, A. P. *Nature* **1999**, *401*, 120–121.

(17) (a) Koumura, N.; Geertsema, E. M.; Meetsma, A.; Feringa, B. L. *J. Am. Chem. Soc.* **2000**, *122*, 12005–12006. (b) Koumura, N.; Geertsema, E. M.; van Gelder, M. B.; Meetsma, A.; Feringa, B. L. *J. Am. Chem. Soc.* **2002**, *124*, 5037–5051.

(18) Geertsema, E. M.; Koumura, N.; ter Wiel, M. K. J.; Meetsma, A.; Feringa, B. L. *Chem. Commun.* **2002**, 2962–2963.

Scheme 1. Retrosynthesis of the New Motor Molecule **3**
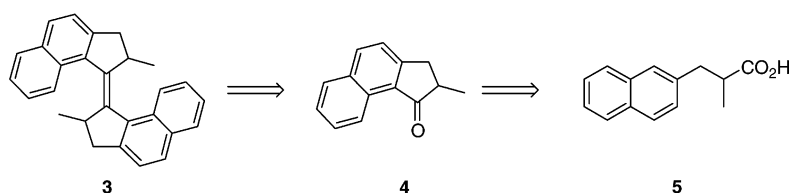
Scheme 2. Synthesis of Motor Molecule **3**
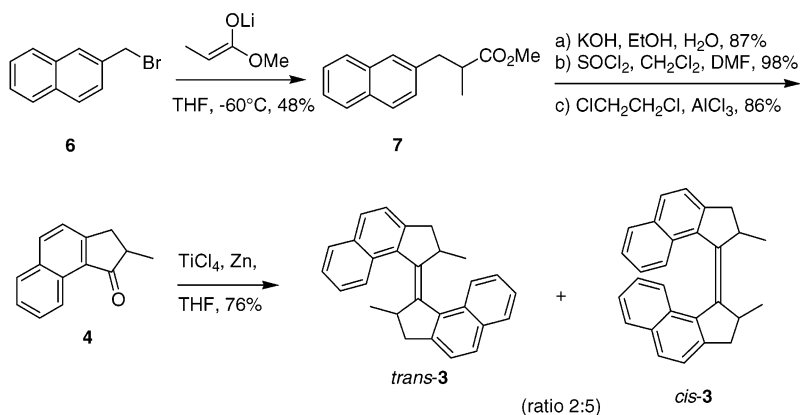
Scheme 3. Asymmetric Synthesis Route toward Motor Molecules **3**
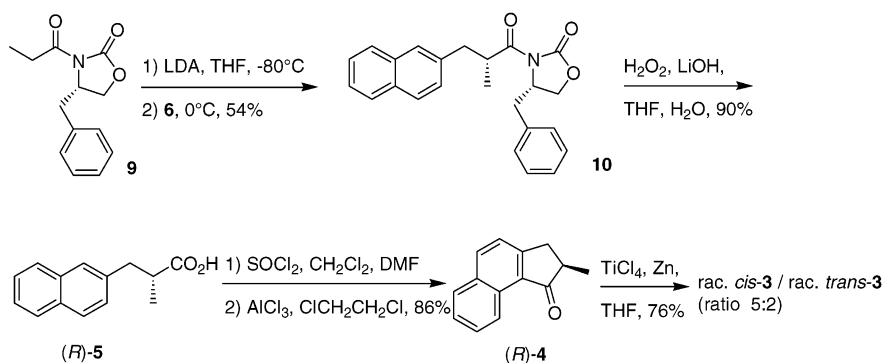
the conformational differences (pseudoaxial or pseudoequatorial) of the methyl substituents at the stereogenic centers in **3** are still large enough to force the movement around the double bond in a unidirectional fashion. A third consideration concerns the photochemical conversions and, in particular, the effect of structural features on the absorption spectra and excited-state geometry. For six-membered ring system **1**, the photoisomerizations have been shown to proceed with high stereoselectivity due to distinct differences in absorption characteristics of the isomers,[16a] but it remains to be seen if this also holds for five-membered analogue **3**.

Synthesis

The synthetic route toward the envisioned molecular motor **3** is dominated by the most crucial step, i.e., the formation of the sterically crowded central olefinic bond via a reductive coupling of two ketones **4** using a McMurry reaction (Scheme 1). The yields of the McMurry coupling[19] of the corresponding ketones of the original motor **1** with six-membered rings were

very low due to steric hindrance.[20] Similar problems can be anticipated for the McMurry coupling of ketone **4** since the two symmetric halves are now connected by a highly sterically demanding double bond between two five-membered rings.

To avoid overalkylation, the methyl substituent is introduced preferably in an early stage of the synthesis. Therefore, the ketones used in the coupling reaction are to be derived from the 2-substituted naphthalene precursor **5**. Ring closure of acid **5** by means of a Friedel−Crafts acylation is supposed to take place regioselectively at the 1-position of the naphthalene moiety to give 2-methyl-2,3-dihydro-1*H*-cyclopenta[*a*]naphthalen-1-one **4**.

The synthesis of **3** is summarized in Scheme 2. The enolate of methyl propionate, generated at low temperature using lithium diisopropylamide as a base, was allowed to react with 2-(bromomomethyl)naphthalene **6** to provide ester **7**. Hydrolysis of ester **7** in a mixture of potassium hydroxide in ethanol and water gave acid **5** which was converted to the corresponding acid chloride **8** followed by ring closure using $AlCl_3$ in dichloro-

(19) For a review on McMurry coupling using low-valent titanium species see: Fürstner, A.; Bogdanović, B. *Angew. Chem., Int. Ed. Engl.* **1996**, *35*, 2442−2469.

(20) (a) Harada, N.; Koumura, N.; Feringa, B. L. *J. Am. Chem. Soc.* **1997**, *119*, 7256−7264. (b) ter Wiel, M. K. J.; Koumura, N.; van Delden, R. A.; Meetsma, A.; Harada, N.; Feringa, B. L. *Chirality* **2000**, *12*, 734−741. (c) ter Wiel, M. K. J.; Koumura, N.; van Delden, R. A.; Meetsma, A.; Harada, N.; Feringa, B. L. *Chirality* **2001**, *13*, 336.
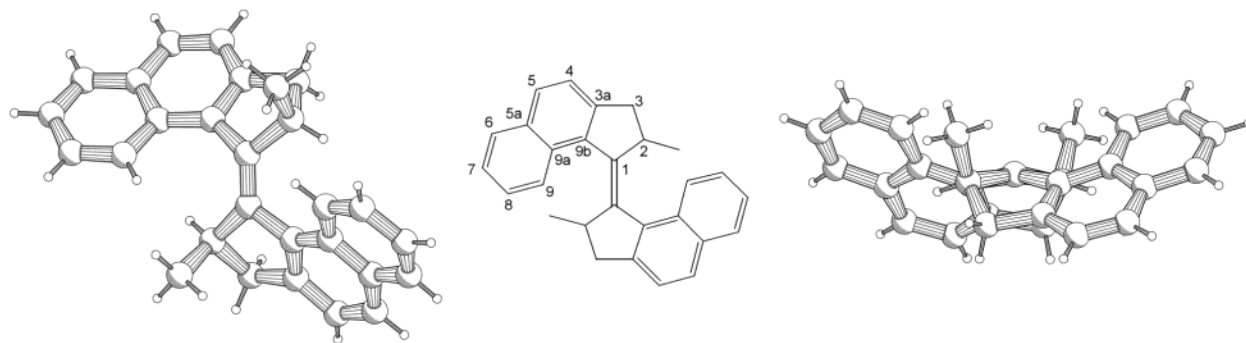
Figure 2. PLUTO drawing of racemic (2R*,2′R*)-(P*,P*)-(E)-(±)-2,2′-dimethyl-2,2′,3,3′-tetrahydro-1,1′-bicyclopenta[a]naphthalenylidene **3**. One enantiomer shown; this structure does not express the absolute stereochemistry of the molecule.

ethane to provide ketone **4** in 86% yield. Finally, reductive coupling of **4** using TiCl$_4$ and Zn provided the overcrowded alkene **3** as a mixture of *cis* and *trans* isomers (ratio 5:2) in a combined yield of 76%. By recrystallization of the *cis−trans* mixture of **3** from ethyl acetate, the pure *trans* isomer was isolated as slightly yellow crystals (mp 192.7−193.2 °C) in 14% yield. Pure *cis* isomer (mp 178.6−179.9 °C) was obtained by repeated recrystallizations from ethanol and ethyl acetate.

Two major differences in the synthesis of **3** compared to that of the original motor molecule have to be mentioned at this point.[20] First, the yield in the reductive coupling of the two ketone moieties is drastically enhanced. Particularly remarkable is the preferred formation of the *cis* isomer in the case of **3**. For the original motor molecule **1**, no *cis* isomer was isolated nor observed by ^{1}H NMR after the McMurry reaction. This could imply that the *cis* isomer of **3** is more stable than the *trans* isomer of **3**. Apparently the stereoselectivity in the formation of the cyclic intermediate during the reductive coupling is affected by the ring size of the ketones.[19]

The alkenes *trans*-**3** and *cis*-**3** were prepared in their racemic forms, and enantioresolution was performed using preparative chiral HPLC. Separation of the enantiomers of the *trans*-**3** alkene proved to be possible on a Daicel Chiralcel OD-column using a highly apolar eluent (heptane:2-propanol = 99.9:0.1). HPLC separation of the enantiomers of the *cis*-**3** was accomplished using heptane:2-propanol = 99.5:0.5 as an eluent on a Daicel Chiralcel OD-column. The configuration of the first eluted fraction of *cis*-**3** was assigned to be (2R,2′R)-(P,P) by comparison with CD data of related compounds (vide infra).

To develop an alternative method to optically active **3**, avoiding time-consuming chromatographic resolution, it was decided to introduce the methyl substituent via an asymmetric synthetic route. In combination with CD spectroscopy this would provide valuable information about the absolute configuration of these molecules. A number of methods have been developed for the stereoselective introduction of an alkyl group next to a carbonyl functional group and for our purpose the methodologies developed by Enders[21] and Evans[22] are particularly relevant. It was decided to use the Evans oxazolidinone protocol which makes use of a less sterically demanding acid derivative and provides methodology that has already proven its value in the synthesis of the six-membered ring analogues.[20b]

The asymmetric synthesis (Scheme 3) starts with chiral oxazolidinone **9** prepared by standard methodology.[23] Generation of the enolate of **9** using LDA followed by quenching with 2-(bromomethyl)naphthalene gives **10** in moderate yield (54%). Since it is possible to form two diastereomers, the reaction mixture was carefully analyzed to ascertain the presence of a diastereomerically pure product. Diastereomerically pure **10** was deprotected using standard conditions to afford carboxylic acid (R)-**5** in high yield (90%). By derivatization of acid (R)-**5** to its methyl ester (R)-**7** the enantiomeric excess of (R)-**5** was determined to be higher than 99% according to HPLC analysis (Daicel Chiralcel OB−H column, heptane:2-propanol = 99:1). Ring closure of acid (R)-**4** by conversion to acid chloride (R)-**8** and subsequent Friedel−Crafts reaction with AlCl$_3$ afforded chiral ketone (R)-**4** in good yield and with high enantiomeric excess. It must be noted that this chiral ketone (R)-**4** is prone to racemization but can be obtained with an ee > 99% according to HPLC analysis (Daicel Chiralcel OB−H column, heptane: 2-propanol = 99:1) using neutral conditions during workup. In the last step, a reductive coupling, using a low-valent titanium species generated by reduction of titanium tetrachloride with zinc powder, provided **3** as a *cis−trans* mixture (ratio 5:2). Chiral HPLC analysis revealed that both isomers of **3** were obtained as racemates. Unfortunately, under the reaction conditions used, the chiral ketone (R)-**4** racemized completely rendering this elegant route, aiming at an asymmetric synthesis of the *cis* and *trans* alkenes, useless for stereoselective formation of enantiomerically pure *cis* and *trans*-**3**.

Structural Analysis

From the ^{1}H and ^{13}C NMR spectra of *cis*-**3** and *trans*-**3** the C$_2$-symmetric nature of both isomers is immediately evident and all NMR data are in complete agreement with the structures of the isomers. The signals in the ^{1}H NMR spectra of *cis*-**3** and *trans*-**3** were assigned individually by COSY and NOESY experiments. In the aromatic region, the ^{1}H NMR spectra of the alkenes *cis*-**3** and *trans*-**3**, with a five-membered ring, closely resemble the ^{1}H NMR absorptions of the corresponding isomers of six-membered alkene **1**.

The proton absorptions in the aromatic region of *trans*-**3** are found at values between δ 7.4 and 8.3 ppm. A confirmation of the *trans*-geometry of the latter molecule is the observation of a NOE interaction between Me2 and H9′ and between H2 and H9′ (for the numbering of *trans*-**3**, see Figure 2). Indicative

(21) Enders, D.; Kipphardt, H.; Fey, P. In *Organic Synthesis*; Vedejs, E., Ed.; John Wiley & Sons: New York, 1987; Vol. 65, pp 183−202.
(22) (a) Evans, D. A.; Ennis, M. D.; Mathre, D. J. *J. Am. Chem. Soc.* **1982**, *104*, 1737−1739. (b) Evans, D. A.; Takacs, J. M.; McGee, L. R.; Ennis, M. D.; Mathre, D. J.; Bartroli, J. *Pure Appl. Chem.* **1981**, *53*, 1109−1127.

(23) Gage, J. R.; Evans, D. A. in *Organic Synthesis*; Freeman, J. P., Ed.; John Wiley & Sons: New York, 1995; Coll. Vol. VIII, pp 528−531.
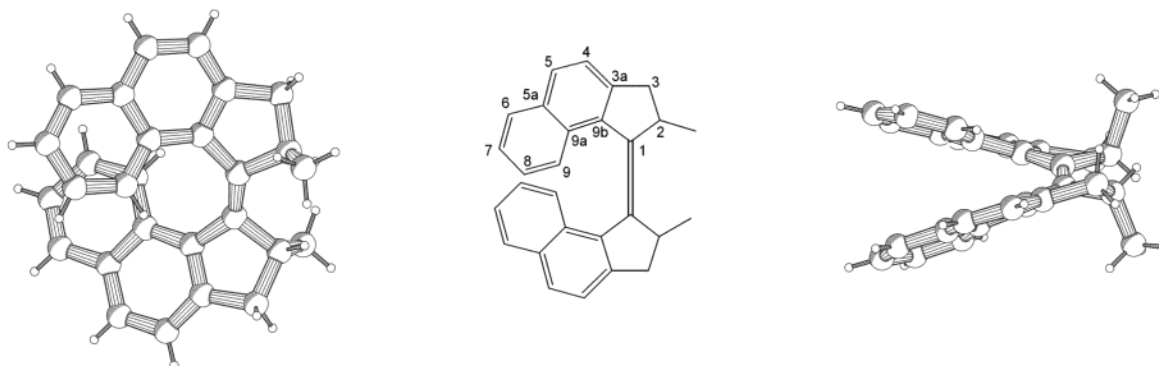
Figure 3. PLUTO drawing of racemic (2R*,2′R*)-(P*,P*)-(Z)-(±)-2,2′-dimethyl-2,2′,3,3′-tetrahydro-1,1′-bicyclopenta[a]naphthalenylidene **3**. One enantiomer shown; this structure does not express the absolute stereochemistry of the molecule.

for the *cis*-**3** isomer are the arene proton absorptions as high as δ 6.4 ppm. The reason for the ^{1}H NMR absorption at relatively high field in *cis*-**3** is the aromatic ring current anisotropy experienced by the close proximity of the naphthalene moiety in the opposite half of the molecule. The upfield shift of the arene protons is in accordance with data of the *cis*-isomer of the six-membered overcrowded alkene described previously.[20a] In the NOESY spectrum of *cis*-**3** no interaction between the Me2 or H2 and H9′ was found (for the numbering of *cis*-**3**, see Figure 3).

To unequivocally prove the molecular geometry and to determine the preferred conformation of the stable forms of these molecules, *trans*-**3** was recrystallized from ethyl acetate to afford crystals suitable for X-ray analysis (Figure 2). The crystal used was found to be orthorhombic with space group *Pbca* (No. 61) and contained one molecule of *trans*-**3** in the asymmetric unit cell.[24] The structure of the compound is slightly distorted due to crystal packing effects but can be regarded pseudo-C_2-symmetric. The most important structural features of *trans*-**3** in the solid state are the overall double helical shape and the (pseudo-)axial orientation of both methyl substituents at the stereogenic centers. As is apparent from Figure 2, the naphthalene moiety and the methyl substituent in one-half of the molecule are pointing in the same direction.

The central double bond in *trans*-**3** was found to be only slightly elongated: 1.3497 Å compared to the literature value of 1.33 Å for a common olefinic bond.[25] The bond angles around C1 and C1′ are as follows: C2−C1−C9b = 104.1°, C2−C1−C1′ = 126.0°, and C9b−C1−C1′ = 127.4°, making the average total angle around C1 and C1′ 357.5° (values are an average of the values found in the two parts of the residue since the structure is being regarded as pseudo C_2-symmetric). Remarkably, in *trans*-**3** the central olefinic bond is more twisted compared to its six-membered analogue **1**. The values for the torsion angles around the double bond are C2−C1−C1′−C2 = −162.2°, C9b−C1−C1′−C9′b = 155.8°, and C2−C1−C1′−C9′b = −3.2° (average). The angle between the least-squares planes of the atoms in both naphthalene moieties (85.2°) in *trans*-**3** shows a close to perpendicular geometry. The twist of the naphthalene moiety itself in *trans*-**3** with respect to the least-

squares plane of the atoms C2−C1−C9b−C9′b−C1′−C2′ is on average 42.6°, a value that is also reflected in the torsion angle C1−C1′−C9′b−C9′a, which is on average 44.5° for both halves of *trans*-**3**. The five-membered ring itself is remarkably flat, and the ring deviates only slightly from the least-squares plane through the atoms C1−C2−C3−C3a−C9b. The atoms C2 and C2′ (average 0.220 Å) and C1 and C1′ (average 0.200 Å) show the largest deviations from this plane. Nevertheless, the methyl substituent at the stereogenic center clearly adopts a (pseudo-)axial orientation (C1−C1′−C2′−Me2ax is −116.2° (average)), and the most stable conformation of *trans*-**3** shows a similar helicity as found for *trans*-**1**.

Suitable crystals for the X-ray structure determination of the racemic *cis*-**3** isomer were obtained by recrystallization from ethanol. The crystal used was found to be monoclinic with space group $P2_1$ (No. 4) and contained two enantiomers of *cis*-**3** in the asymmetric unit cell.[24] The two residues (from hereon arbitrarily named enantiomer 1 and 2) are, apart from minor distortions due to crystal packing effects, enantiomers of each other.

Similar to *trans*-**3**, the structure of *cis*-**3** is C_2-symmetric at first sight, but both residues are slightly distorted. Clearly, the helical shape and the (pseudo-)axial orientation of the methyl substituents at the stereogenic centers can be seen from the structure depicted in Figure 3. Both the naphthalene moiety and the methyl substituent in each half are pointing in the same direction, implying that this geometry is the most stable for *cis*-**3**. The central double bonds in both enantiomers of *cis*-**3** (1.365 and 1.352 Å) were found to be more elongated and flatter than the central double bond in *trans*-**3** (1.3497 Å). The bond angles around C1 and C1′ in enantiomer 1 are as follows: C2−C1−C9b = 105.0°, C2−C1−C1′ = 121.6°, and C9b−C1−C1′ = 133.2° (average total angle around C1 and C1′ = 359.8°); in enantiomer 2 they are as follows: C2−C1−C9b = 104.6°, C2−C1−C1′ = 122.0°, and C9b−C1−C1′ = 133.3° (average total angle around C1 and C1′ = 359.9°) (values are an average of the values found in the two parts of the residue since the structure is pseudo C_2-symmetric). The values for the torsion angles around the double bond are as follows: C2−C1−C1′−C2 = 11.0°, C9b−C1−C1′−C9′b = −3.2°, and C2−C1−C1′−C9′b = −176.1° (average) for enantiomer 1 and C2−C1−C1′−C2 = −10.9°, C9b−C1−C1′−C9′b = 1.4°, and C2−C1−C1′−C9′b = 175.3° for enantiomer 2. This means that the deviation from planarity of the central double bond for *cis*-**3** is smaller than was found for both *trans*-**1** and *trans*-**3**. In *cis*-**3** the angle

(24) X-ray crystallographic data and details of the structure determination are listed in Table 1 in the Supporting Information. The numbering of the atoms adopted in both X-ray structures is according to IUPAC rules in this paper. Since this numbering is different in the cif file, tables in the Supporting Information are included to convert the labels used.

(25) *CRC Handbook of Chemistry and Physics 1993−1994*; Lide, D. R., Ed.; CRC Press: Boca Raton, FL, 1993; Vol. 74, pp 9−4.
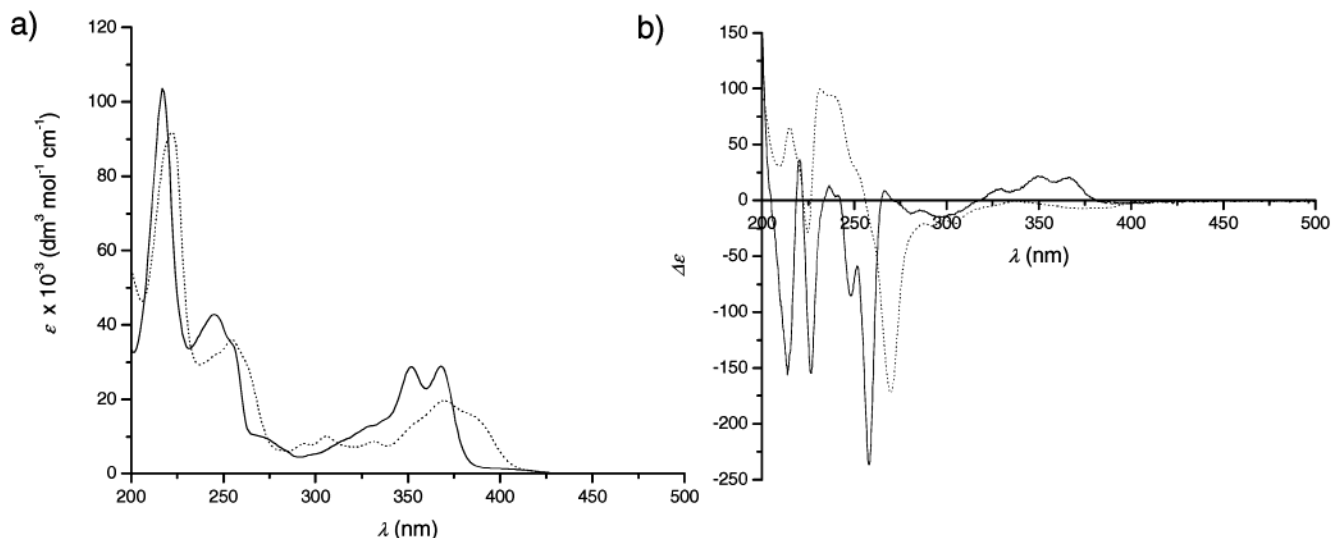
Figure 4. (a) UV−vis spectra (*n*-hexane) of the stable olefins: *cis*-**3** (dotted line) and *trans*-**3** (solid line); (b) CD spectra (*n*-hexane) of the stable olefins: (2*R*,2′*R*)-(*P,P*)-*cis*-**3** (dotted line) and (2*R*,2′*R*)-(*P,P*)-*trans*-**3** (solid line).

between the least-squares planes of the atoms in both naphthalene moieties (average 31.5°) was much smaller than for *trans*-**3** (85.2°). This is reflected in the torsion angles in both enantiomers between C1′−C1−C9b−C9a which are 31.3° and −32.7°, respectively, in *cis*-**3**. Again, the five-membered ring itself is remarkably flat and its atoms deviate only slightly from the plane through C1−C2−C3−C3a−C9b in both moieties; the largest deviations are associated with the atoms C1, C2, C1′, and C2′. However, the five-membered ring in *cis*-**3** is even more planar than that of *trans*-**3**, the average deviation of C1 and C1′ in both residues being 0.172 Å and of C2 and C2′ 0.185 Å. Also, for *cis*-**3**, it is clear that the methyl substituents at the stereogenic center adopt a (pseudo-)axial orientation (C1−C1′−C2′−Me2ax are on average −96.4° and 96.9°).

Photochemical Experiments

Enantiomerically pure (2*R*,2′*R*)-(*P,P*)-*cis*-**3**, obtained by preparative chiral HPLC, was irradiated at −40 °C in *n*-hexane and subsequently heated at room-temperature resulting in a mixture of (2*R*,2′*R*)-(*P,P*)-*cis*-**3** and (2*R*,2′*R*)-(*P,P*)-*trans*-**3** (vide infra). These two isomers were readily separated by chiral HPLC on a preparative Daicel Chiralcel OD-column (heptane:*i*-propanol = 99.9:0.1). The UV−vis spectra of pure *cis*-**3** and *trans*-**3** are shown in Figure 4a, and the circular dichroism (CD) spectra of enantiomerically pure (2*R*,2′*R*)-(*P,P*)-*cis*-**3** and (2*R*,2′*R*)-(*P,P*)-*trans*-**3** are shown in Figure 4b. The absolute configuration of (2*R*,2′*R*)-(*P,P*)-*cis*-**3** and (2*R*,2′*R*)-(*P,P*)-*trans*-**3** could be assigned by comparison of CD data with the CD spectra of (3*R*,3′*R*)-(*P,P*)-*cis*-**1** and (3*R*,3′*R*)-(*P,P*)-*trans*-**1**.[16a,20] The orientation of methyl substituent at the stereogenic centers was confirmed to be (pseudo-)axial, as was apparent by X-ray structural analysis of *cis*-**3** and *trans*-**3** (vide supra).

The anticipated four-step unidirectional rotation of **3** is depicted in Scheme 4. On the basis of our experience with **1** and related molecular motors, irradiation of the stable (2*R*,2′*R*)-(*P,P*)-*cis*-**3** is expected to result in the formation of the energetically unfavored (2*R*,2′*R*)-(*M,M*)-*trans*-**3** isomer where the methyl substituents are forced to adopt a (pseudo-)equatorial orientation (step 1). Heating of (2*R*,2′*R*)-(*M,M*)-*trans*-**3** should induce a thermal helix inversion to form the stable (2*R*,2′*R*)-

Scheme 4. Photochemical and Thermal Isomerization Processes during 360° Unidirectional Rotary Cycle
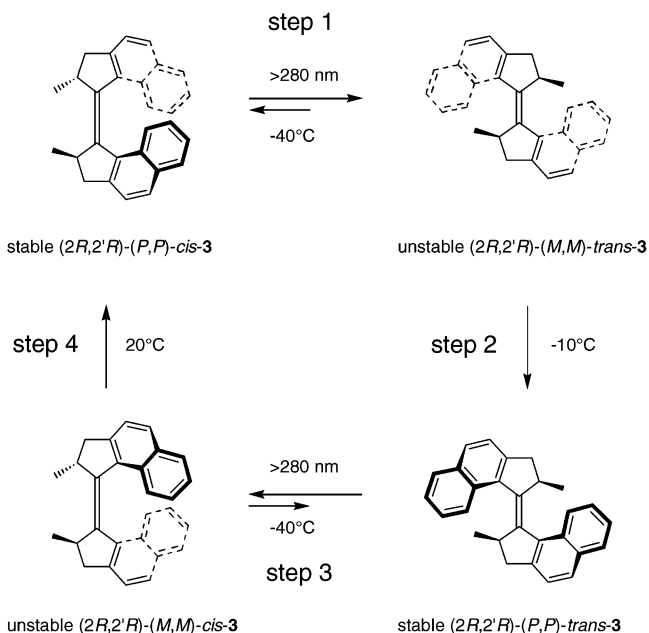
(*P,P*)-*trans*-**3** (step 2). A second energetically uphill photo-isomerization (step 3) followed by a thermal helix inversion (step 4) should complete a four-step 360° unidirectional rotation.

Photoisomerization of a sample of (2*R*,2′*R*)-(*P,P*)-*cis*-**3** in *n*-hexane by irradiation with $\lambda \geq 280$ nm at −40 °C was monitored by UV−vis (Figure 5a) and CD spectroscopy (Figure 5b). The major band in the CD spectrum shifted from 270.0 nm for the initial (2*R*,2′*R*)-(*P,P*)-*cis*-**3** to 263.2 nm at the photostationary state (PSS) and changed sign from $\Delta\epsilon = -172.2$ to $\Delta\epsilon = 13.1$ (Figure 5b). The change in sign of the CD signal is indicative for the helix inversion of the molecule going from a overall (*P*)-helicity in (2*R*,2′*R*)-(*P,P*)-*cis*-**3** to an (*M*)-helicity in the newly formed isomer, anticipated to be the energetically unstable (2*R*,2′*R*)-(*M,M*)-*trans*-**3** isomer with both methyl substituents in an equatorial orientation (step 1, Scheme 4). The exact nature of this unstable *trans*-isomer was confirmed by low-temperature ¹H NMR. A solution of racemic stable *cis*-**3**
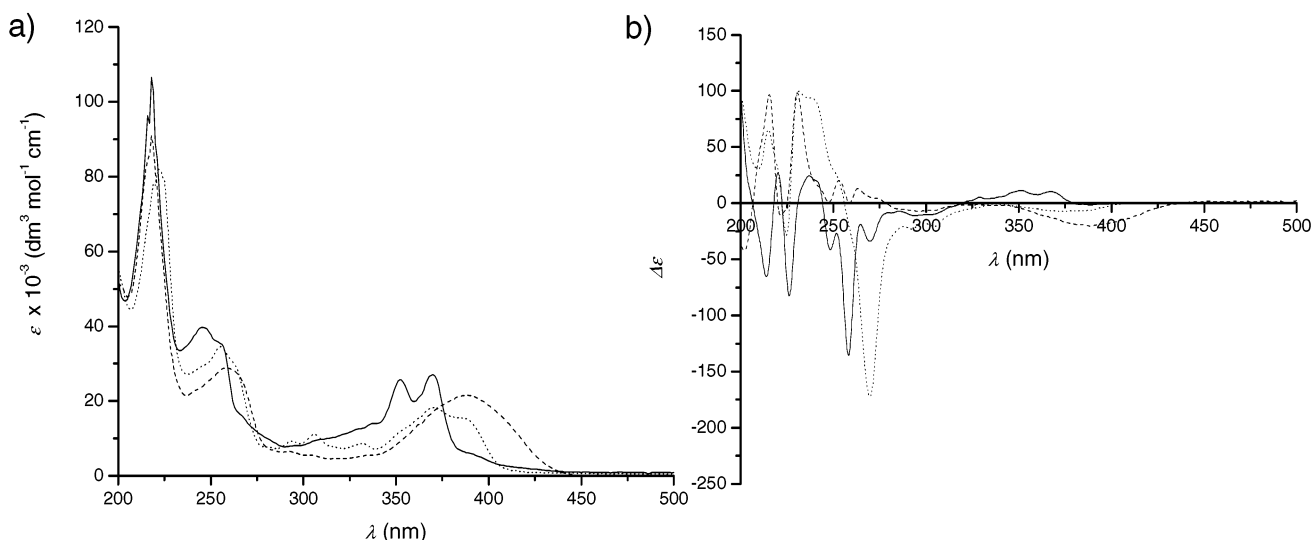
Figure 5. UV-vis (*n*-hexane) (a) and CD spectra (*n*-hexane) (b) of the first half of the rotary cycle: pure (2*R*,2′*R*)-(*P*,*P*)-*cis*-**3** (dotted line), after step 1 (dashed line), and after step 2 (solid line) (cf. Scheme 4).
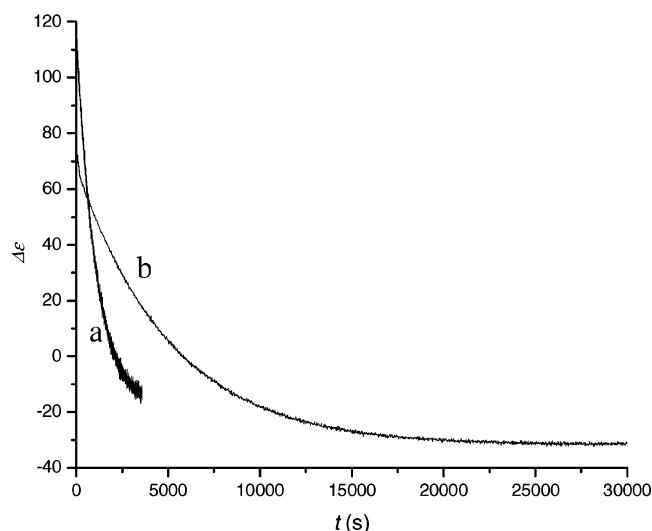

Figure 6. CD absorptions monitored in time for the two thermal helix conversions in the rotary process: (a) conversion of (2*R*,2′*R*)-(*M*,*M*)-*trans*-**3** to (2*R*,2′*R*)-(*P*,*P*)-*trans*-**3** (Δε at 230 nm, −10 °C, *n*-hexane); (b) conversion of (2*R*,2′*R*)-(*M*,*M*)-*cis*-**3** to (2*R*,2′*R*)-(*P*,*P*)-*cis*-**3** (Δε at 279 nm, 20 °C, *n*-hexane).

(toluene-*d*₈), with methyl groups in an axial orientation, was irradiated overnight at −78 °C ($\lambda \geq 280$ nm). Upon irradiation, the signals of the methyl protons of stable *cis*-**3** at δ 1.17−1.18 ppm shifted to higher field at δ 0.68−0.69 ppm as a result of the diequatorial orientation of the methyl groups in unstable *trans*-**3** formed. In the aromatic part of the spectrum, signals appeared at lower field, 7.70−7.72 and 7.95−7.97 ppm, indicative of the formation of a molecule with a *trans* conformation. Heating of this sample showed a clean conversion of unstable *trans*-**3**, with equatorial methyl groups, to stable *trans*-**3**, with axial methyl groups.

Subsequently the irradiated *n*-hexane solution, containing the photostationary state mixture of (2*R*,2′*R*)-(*P*,*P*)-*cis*-**3** and (2*R*,2′*R*)-(*M*,*M*)-*trans*-**3**, was kept at −10 °C and the CD signal at 230 nm was monitored in time. An inversion of the CD spectrum was observed after complete conversion, indicating the overall inversion of helicity of the molecule (Figure 5b and Figure 6, trace a). This indicates that unstable (2*R*,2′*R*)-(*M*,*M*)-*trans*-**3** was

converted to stable (2*R*,2′*R*)-(*P*,*P*)-*trans*-**3** (step 2, Scheme 4). In (2*R*,2′*R*)-(*P*,*P*)-*trans*-**3** the methyl substituents of the molecule are back in their favored (pseudo-)axial conformation. From the change in CD monitored in time, the rate constant (k_t) at various temperatures was determined and subsequently used to calculate the Gibbs free energy of activation ($\Delta G^{\theta\ddagger} = 80 \pm 1$ kJ·mol^{-1}) using the Eyring equation. This means that the conversion of (2*R*,2′*R*)-(*M*,*M*)-*trans*-**3** to (2*R*,2′*R*)-(*P*,*P*)-*trans*-**3** has a half-life of only 18 s at room temperature (293.15 K).

Due to the low stability of (2*R*,2′*R*)-(*M*,*M*)-*trans*-**3**, the PSS ratio of the first photoequilibrium could not be determined directly. After the thermal conversion of (2*R*,2′*R*)-(*M*,*M*)-*trans*-**3** to (2*R*,2′*R*)-(*P*,*P*)-*trans*-**3**, the amount of stable (2*R*,2′*R*)-(*P*,*P*)-*trans*-**3** formed reflects the amount of unstable (2*R*,2′*R*)-(*M*,*M*)-*trans*-**3** at the PSS. Using chiral HPLC analysis, the ratio of (2*R*,2′*R*)-(*P*,*P*)-*cis*-**3** and (2*R*,2′*R*)-(*M*,*M*)-*trans*-**3** at the PSS mixture was determined to be 22:78. The formation of (2*R*,2′*R*)-(*P*,*P*)-*trans*-**3** was confirmed by comparison with racemic and enantiomerically pure (2*R*,2′*R*)-(*P*,*P*)-*trans*-**3**. From these data, the CD and UV−vis spectra of unstable (2*R*,2′*R*)-(*M*,*M*)-*trans*-**3** could be calculated (Figure 7).

The mixture of (2*R*,2′*R*)-(*P*,*P*)-*cis*-**3** and (2*R*,2′*R*)-(*P*,*P*)-*trans*-**3** (22:78 ratio) obtained after irradiation and heating of the original sample was used for further experiments. Irradiation of this sample ($\lambda \geq 280$ nm at −40 °C), resulted in a change of the sign of the CD signal and the major band in the CD spectrum shifted from 258.4 to 279.0 nm and changed sign from $\Delta\epsilon = -135.6$ to $\Delta\epsilon = 59.1$ (Figure 8). This is indicative of the helix inversion taking place upon irradiation of (2*R*,2′*R*)-(*P*,*P*)-*trans*-**3** and (2*R*,2′*R*)-(*P*,*P*)-*cis*-**3** to (2*R*,2′*R*)-(*M*,*M*)-*cis*-**3** and (2*R*,2′*R*)-(*M*,*M*)-*trans*-**3**, respectively. Due to low stability of the diequatorial compounds the ratio of the four forms present in the mixture could not be determined directly. Confirmation of the structure of the racemic unstable *cis*-**3** with equatorial methyl groups was also performed by low-temperature ¹H NMR. A sample of racemic stable *trans*-**3** with methyl groups in an axial orientation, dissolved in toluene-*d*₈, was irradiated overnight at −78 °C ($\lambda \geq 280$ nm). Due to a diequatorial orientation of the methyl groups in the unstable *cis*-**3** formed, a new doublet appeared at lower field (δ 1.46−1.47 ppm) compared to the
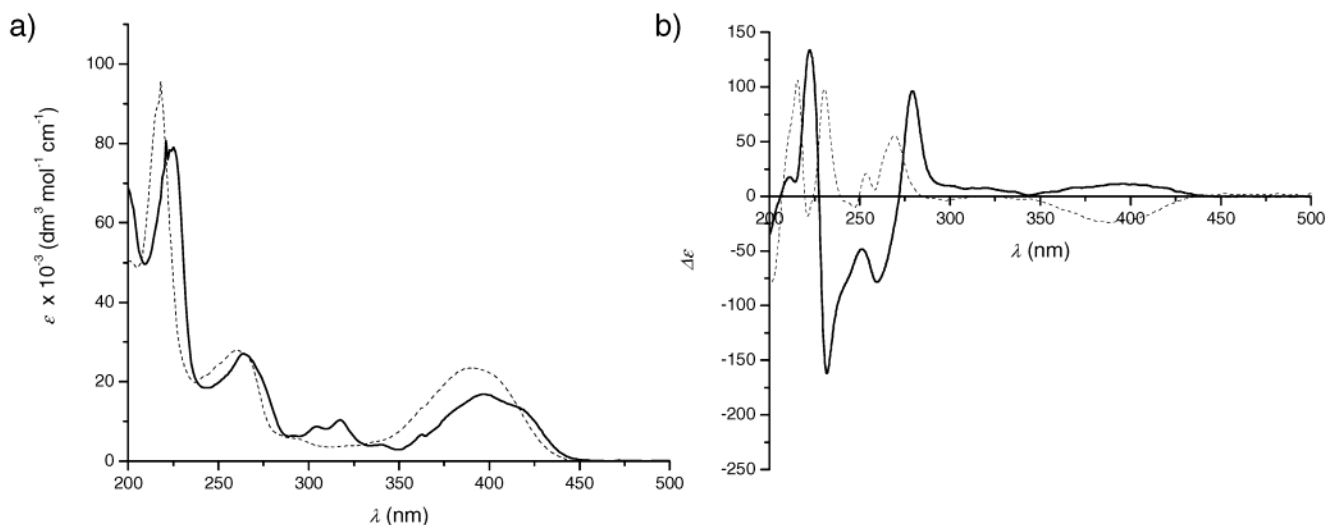
Figure 7. Calculated UV–vis (*n*-hexane) (a) and CD spectra (*n*-hexane) (b) of (2R,2′R)-(M,M)-*trans*-**3** (dashed line) and (2R,2′R)-(M,M)-*cis*-**3** (thick solid line).
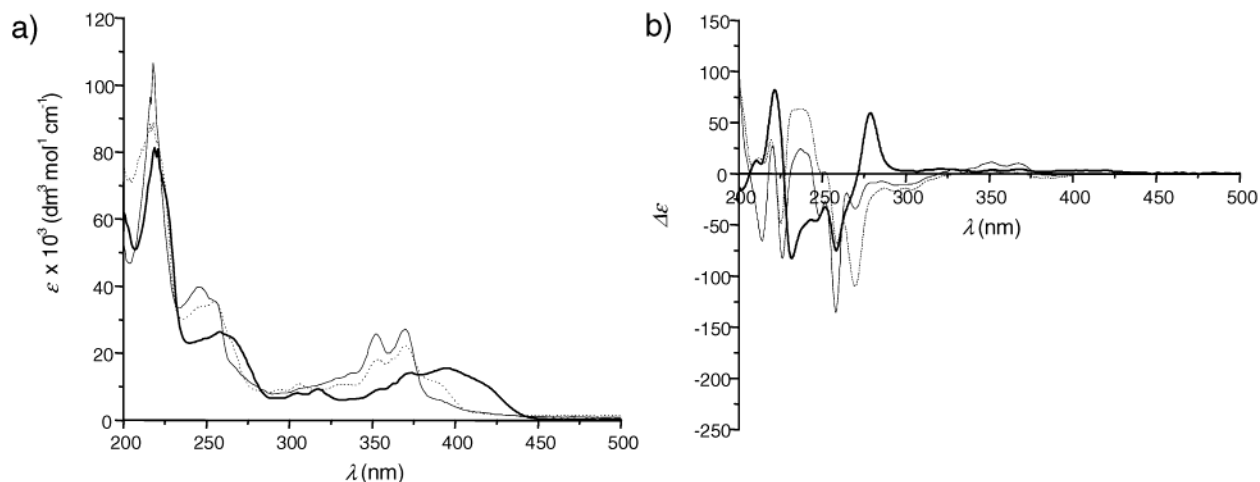

Figure 8. UV–vis (*n*-hexane) (a) and CD spectra (*n*-hexane) (b) of the second half of the rotary cycle: after step 2 (solid line), step 3 (thick solid line), and step 4 (short dotted line).

signals of the protons of the methyl groups of stable *trans*-**3** (δ 1.26–1.27 ppm). In the aromatic region of the spectrum, absorptions appeared at higher field, δ 6.49–6.52 and 6.75–6.78 ppm, which is indicative for the shielded protons due to the anisotropic ring current in a compound with *cis* conformation. After heating of this sample, a clean conversion of the unstable *cis*-**3** with equatorial methyl groups to the stable *cis*-**3** with axial methyl groups was observed.

After the photoirradiation the CD signal of the sample was monitored in time at 279 nm at 20 °C during which an inversion of the CD signal was observed due to thermal helix inversion taking place (Figure 6, trace b). The equilibrium ratio of (2R,2′R)-(P,P)-*cis*-**3** and (2R,2′R)-(P,P)-*trans*-**3** was determined by HPLC to be 67:33. Taking into account the ratio established for the first photoequilibrium, for the second photoequilibrium can be calculated a PSS ratio of (2R,2′R)-(P,P)-*trans*-**3** and (2R,2′R)-(M,M)-*cis*-**3** of 21:79. From time-dependent CD measurements, the rate constants k_c of the first-order process were obtained at various temperatures. These data were used to calculate both the Gibbs free energy of activation ($\Delta G^{\theta\ddagger} = 93 \pm 1$ kJ·mol^{-1}) and the half-life of this helix inversion at room temperature ($t_{1/2} = 74$ min, 293.15K). Using these data, the CD

and UV–vis spectra of unstable (2R,2′R)-(M,M)-*cis*-**3** could be calculated (Figure 7).

The CD spectra of (2R,2′R)-(P,P)-*cis*-**3** (Figure 4b) and (2R,2′R)-(M,M)-*cis*-**3** (Figure 7b) and (2R,2′R)-(P,P)-*trans*-**3** (Figure 4b) and (2R,2′R)-(M,M)-*trans*-**3** (Figure 7b) nicely show the pseudoenantiomeric relation between the stable and less stable forms of both *cis*-**3** and *trans*-**3**. Comparing the CD spectra of both forms of the *cis*-**3** and *trans*-**3** isomers, there is a net inversion of the major absorptions. However, the stepwise inversions of the CD signals in the rotary cycle of the five-membered ring motor molecule are less pronounced than was the case for the six-membered ring motor molecule. Although the intensity and the shape of the CD spectra of all four isomers is sufficiently different to show the helix inversion in each step, as shown in Figures 5b and 8b, the effect is less pronounced due to the less favorable photoequilibria for the motor system **3**.

The ratios of the PSS of the first step of the molecular motor **1**, going from stable *trans*-**1** to unstable *cis*-**1**, and for the third step, going from stable *cis*-**1** to unstable *trans*-**1**, were 5:95 and 10:90, respectively.[16a] The corresponding ratios of the molecular motor **3** are 22:78 for the first step, going from stable *cis*-**3** to

unstable *trans*-**3**, and 21:79 for the third step in the rotary process, going from stable *trans*-**3** to unstable *cis*-**3**. It should be emphasized that the slightly lower selectivity does not affect the unidirectional rotation as long as light energy is supplied and the temperature is sufficiently high to ensure thermal helix inversion. The thermal barriers, which are the rate-determining steps in the rotary process, have decreased considerably, and molecular motor **3** can perform its 360° rotation readily at room temperature. This is a significant improvement compared to the first-generation molecular motor **1** which has to be heated at 60 °C before a significant conversion of the unstable *trans*-form to the stable *trans*-form takes place. Even compared to most of the so-called second-generation molecular motors,[17b] where the speed of rotation could be tuned by synthetic modification, the newly presented motor molecule **3** is very fast. There is only one molecule of the nonsymmetric six-membered ring molecular motors which can keep up with the speed of the current symmetrical five-membered motor molecule **3**. The unstable form of the fastest rotating second-generation motor molecule has an half-life of 40 min at room temperature, which is slightly faster than the slowest step going from unstable *cis*-**3** to stable *cis*-**3** ($t_{1/2} = 74$ min) but much slower than the fastest step going from unstable *trans*-**3** to stable *trans*-**3** ($t_{1/2} = 18$ s). The fact that the symmetrical five-membered motor molecule **3** shows much faster rotary motion than the (symmetrical) six-membered molecules **1** and **2** in the thermally driven helix inversions is promising for the further development of even faster, new generations of motor molecules. Moreover, it is highly surprising that compound **3,** which has two nearly flat five-membered rings, can have two energetically distinct conformations and that the apparently rather small differences in orientation of its methyl substituents are able to control the unidirectional rotation process.

Conclusions

The new molecular motor **3** presented here has a five-membered ring in both the upper and lower halves connected by an olefinic bond, a structural feature distinct from all light-driven molecular motors reported so far which contain either one or two six-membered rings. The new molecular motor **3** is far more efficiently synthesized as yields of up to 76% have been reached in the coupling reaction. A remarkable finding is that, in contrast to the synthesis of the symmetrical molecular motor **1**, both *cis* and *trans* isomers of **3** are obtained. The *cis*-isomer of **3** is even obtained in excess, whereas during the preparation **1** no trace amount of a *cis*-isomer was found. Photoisomerization studies with **3** revealed that the photochemical equilibria are less favorable compared to molecular motors with a six-membered ring. Both the five- and six-membered molecular motors have a similar geometry as far as the overall helicity and stereochemistry of the molecule is concerned. X-ray crystallographic analysis showed that the atoms in the five-membered ring have only a slight deviation of the least-squares plane through the five-membered ring. As a result there are only small conformation differences between the methyl substituents in a (pseudo-)axial and in a (pseudo-)equatorial orientation, but surprisingly the energy differences are still large enough to enable the molecule to rotate in a unidirectional fashion. The unidirectionality of the rotation has been proven by CD spectroscopy and ^{1}H NMR at low temperature. Compared to the symmetric first-generation molecular motor **1**, the newly

presented motor **3** is considerably faster, and only one second-generation molecular motor with a six-membered ring can keep up with the present molecular system. Because of the low thermal isomerization barriers, molecular motor (2*R*,2′*R*)-**3** is capable of a continuous rotation in a net clockwise fashion upon irradiation at room temperature. The slightly lower selectivity of both photoisomerizations does not affect the unidirectional rotary motion since the two thermal inversion steps shift both photoequilibria under conditions of continuous irradiation. The presented findings offer important guidelines for the design of more advanced rotary motors.

Experimental Section

General Procedure. ^{1}H NMR spectra were recorded on a Varian Gemini VXR-300 (300 MHz) or on a Varian Unity Plus (500 MHz). ^{13}C NMR spectra were recorded on a Varian Gemini-200 or a Varian VXR-300 operating at 50.32 or 75.48 MHz, respectively. Chemical shifts are denoted in δ-unit (ppm) relative to $CDCl_3$ (7.26 ppm) and toluene-d_8 (2.08 ppm). The splitting parameters are designated as follows: s (singlet), d (doublet), t (triplet), q (quartet), m (multiplet), and b (broad) for ^{1}H NMR. For ^{13}C NMR, the carbon atoms are assigned as q (primary carbon), t (secondary carbon), d (tertiary carbon), s (quaternary carbon). Melting points were taken on a Mettler FP-2 melting point apparatus, equipped with a Mettler FP-21 microscope and are uncorrected. Optical rotations were measured with a Perkin-Elmer 241 Polarimeter. UV measurements were performed on a Hewlett-Packard HP 8453 FT spectrophotometer, and CD spectra were recorded on a JASCO J-715 spectropolarimeter using Uvasol-grade solvents (Merck). MS (EI) and HRMS (EI) spectra were obtained with a JEOL JMS-600 spectrometer. Column chromatography was performed on silica gel (Aldrich 60, 230−400 mesh). HPLC analyses were performed on Shimadzu HPLC system equipped with two LC-10AD*vp* solvent delivery systems, a DGU-14A degasser, a SIL-10AD*vp* autosampler, a SPD-M10A UV−vis photodiode array detector, a CTO-10A*vp* column oven, and a SCL-10A*vp* controller unit using Chiralcel OD (Daicel) and Chiralcel OB-H (Daicel) columns. Preparative HPLC was performed on a Gilson HPLC system consisting of a 231XL sampling injector, a 306 (10SC) pump, an 811C dynamic mixer, a 805 manometric module, with a 119 UV−vis detector, and a 202 fraction collector, using the Chiralcel OD (Daicel) column. Elution speed was 1 mL/min. Solvents were distilled and dried before use by standard methodology. Chemicals were used as received from Acros, Aldrich, Fluka, or Merck. Irradiation experiments were performed with a 180 W Oriel Hg-lamp using a Pyrex filter. Photostationary states were ensured by monitoring composition changes in time by taking UV spectra at distinct intervals until no changes were observed. Thermal helix inversions were monitored by CD spectroscopy using the apparatus described above and a JASCO PFD-350S/350L Peltier-type FDCD attachment with a temperature control.

(2*R**,2′*R**)-(*P**,*P**)-(*E*)-(±)- and (2*R**,2′*R**)-(*P**,*P**)-(*Z*)-(±)-2,2′-Dimethyl-2,2′,3,3′-tetrahydro-1,1′-bicyclopenta[*a*]naphthalenyli-dene 3. To a stirred suspension of zinc powder (1.34 g, 20.5 mmol) in THF (6 mL) was added slowly at 0 °C $TiCl_4$ (1.14 mL, 10.3 mmol). The resulting black slurry was then heated at reflux for 2 h. A solution of ketone **4** (1.01 g, 5.15 mmol) in THF (4 mL) was added, and the heating was continued for 3 days. The reaction mixture was poured into a saturated aqueous solution of NH_4Cl (100 mL) and was extracted with ethyl acetate (3 × 75 mL). The combined organic layers were dried ($MgSO_4$), and the solvents were removed under reduced pressure to yield the impure product as a brown oil. Further purification was performed by column chromatography (SiO_2, heptane, $R_f = 0.31$), yielding the desired olefins as a yellowish oil (605 mg, 1.96 mmol, 76%) as a mixture of *cis*-**3** and *trans*-**3** in an approximate ratio of 5:2. The *trans*-**3** olefin could be recrystallized from ethyl acetate to provide beige crystals in 14% yield (mp 192.7−193.2 °C). For the purification

of the *cis*-**3** olefin, multiple recrystallizations from ethyl acetate and ethanol were required before obtaining it pure as slightly yellow crystals (mp 178.6−179.9 °C); *m/z* (EI, %) = 360 (M^+, 100). HRMS (EI): calcd. for $C_{28}H_{24}$ 360.1878, found 360.1866. Resolution of *cis*-**3** was performed by chiral HPLC using a Daicel Chiralcel OD column as the stationary phase and a mixture of heptane:2-propanol in a ratio of 99.5:0.5 as the eluent at a rate of 1 mL/min. The first eluted fraction (*t* = 4.89 min) of *cis*-**3** contained (2*R*,2′*R*)-(*P,P*)-(*Z*)-**3**, and the second fraction (*t* = 6.12 min) contained (2*S*,2′*S*)-(*M,M*)-(*Z*)-**3**. Both *trans*-**3** isomers have the same retention time (*t* = 5.54 min) using heptane:2-propanol in a ratio of 99.5:0.5 as the eluent. The *trans*-**3** isomer could be separated using a Chiralcel OD column as the stationary phase and a mixture of heptane:2-propanol in a ratio of 99.9:0.1 as the eluent at a rate of 1 mL/min. The retention times of the enantiomers were *t* = 12.2 and 14.4 min, respectively. The first eluted fraction of *trans*-**3** contained (2*R*,2′*R*)-(*P,P*)-(*E*)-**3**, and the second fraction contained (2*S*,2′*S*)-(*M,M*)-(*E*)-**3**. By irradiation of an enantiomerically pure solution of (2*R*,2′*R*)-(*P,P*)-(*Z*)-3 in *n*-hexane at −40 °C and subsequent heating, a mixture of (2*R*,2′*R*)-(*P,P*)-(*Z*)-**3** and (2*R*,2′*R*)-(*P,P*)-(*E*)-3 was obtained, which was separated using preparative HPLC (Daicel Chiralcel OD column as the stationary phase and a mixture of heptane:2-propanol in a ratio of 99.9:0.1 as the eluent at a rate of 1 mL/min) into the individual compounds. *Racemic stable trans*-**3**: ^{1}H NMR (300 MHz, CDCl$_3$) δ: 1.29−1.32 (d, *J* = 6.2 Hz, 6H, Me2ax), 2.32−2.37 (d, *J* = 14.7 Hz, 2H, H3eq), 2.93−3.00 (dd, *J* = 14.7, 5.5 Hz, 2H, H3ax), 3.03−3.09 (m, 2H, H2eq), 7.39−7.42 (d, *J* = 8.1 Hz, 2H, H4), 7.44−7.49 (m, 2H, H7), 7.52−7.57 (m, 2H, H8), 7.75−7.78 (d, *J* = 8.1 Hz, 2H, H5), 7.90−7.93 (d, *J* = 8.4 Hz, 2H, H6), 8.25−8.27 (d, *J* = 8.4 Hz, 2H, H9). ^{1}H NMR (500 MHz, C$_7$D$_8$, −20 °C) δ: 1.26−1.27 (d, *J* = 6.4 Hz, 6H), 2.04−2.07 (d, *J* = 14.6 Hz, 2H), 2.72−2.76 (dd, *J* = 14.6, 5.6 Hz, 2H), 3.07−3.10 (m, 2H), 7.18−7.20 (d, *J* = 8.2 Hz, 2H), 7.30−7.33 (m, 2H), 7.38−7.41 (m, 2H), 7.56−7.58 (d, *J* = 8.1 Hz, 2H), 7.72−7.74 (d, *J* = 8.1, 2H), 8.38−8.39 (d, *J* = 8.1 Hz, 2H). ^{13}C NMR (50.32 MHz, CDCl$_3$) δ: 19.3 (q), 41.3 (t), 43.1 (d), 124.1 (d), 124.7 (d), 125.0 (d), 126.7 (d), 127.7 (d), 128.4 (d), 130.2 (s), 132.9 (s), 138.5 (s), 141.4 (s), 141.8 (s). UV−vis (*n*-hexane) $\lambda_{max}(\epsilon)$: 217 (103 600), 245 (42 900), 352 (28 700), 368 (29 000). *Racemic stable cis*-**3**: ^{1}H NMR (300 MHz, CDCl$_3$) δ: 1.22−1.24 (d, *J* = 6.6 Hz, 6H, Me2ax), 2.66−2.71 (d, *J* = 14.7 Hz, 2H, H3eq), 3.56−3.65 (m, 4H, H2eq, H3ax), 6.34−6.39 (m, 2H, H8), 6.57−6.60 (d, *J* = 8.4 Hz, 2H, H9), 6.94−6.99 (m, 2H, H7), 7.47−7.50 (d, *J* = 8.1 Hz, 2H, H4), 7.64−7.66 (d, *J* = 8.1 Hz, 2H, H6), 7.70−7.72 (d, *J* = 8.1 Hz, 2H, H5). ^{1}H NMR (500 MHz, C$_7$D$_8$, −20 °C) δ: 1.17−1.18 (d, *J* = 6.5 Hz, 6H), 2.46−2.49 (d, *J* = 15.0 Hz, 2H), 3.38−3.42 (dd, *J* = 15.0, 6.0 Hz, 2H), 3.45−3.48 (m, 2H), 6.35−6.38 (m, 2H), 6.80−6.83 (m, 2H), 7.34−7.36 (d, *J* = 8.1 Hz, 2H), 7.50−7.51 (d, *J* = 8.1 Hz, 2H), 7.57−7.59 (d, *J* = 7.7 Hz, 2H); one aromatic (d) was not observed due to overlap with the solvent. ^{13}C NMR (75.48 MHz, CDCl$_3$) δ: 20.7 (q), 40.6 (t), 42.2 (d), 123.5 (d), 124.0 (2xd), 126.7 (d), 127.6 (d), 128.4 (d), 129.9 (s), 132.2 (s), 136.9 (s), 140.0 (s), 144.0 (s). UV−vis (*n*-hexane) $\lambda_{max}(\epsilon)$: 222 (91 900), 255 (36 000), 294 (8100), 306 (10 100), 332 (8600), 370 (19 600). *Racemic unstable trans*-**3**: ^{1}H NMR (500 MHz, C$_7$D$_8$, −20 °C) δ: 0.68−0.69 (d, *J* = 6.0 Hz, 6H), 2.76−2.81 (dd, *J* = 15.0, 7.7 Hz, 2H), 2.94−2.98 (dd, *J* = 15.0, 7.7 Hz, 2H), 3.45−3.48 (m, 2H), 7.24−7.26 (d, *J* = 7.7 Hz, 2H), 7.28−7.31 (m, 2H), 7.36−7.38 (m, 2H), 7.59−7.61 (d, *J* = 8.1 Hz, 2H), 7.71−7.73 (d, *J* = 7.7 Hz, 2H), 7.95−7.97 (d, *J* = 8.6 Hz, 2H). *Racemic unstable cis*-**3**: ^{1}H NMR (500 MHz, C$_7$D$_8$, −20 °C) δ: 1.46−1.47 (d, *J* = 6.0 Hz, 6H), 2.93−2.97 (dd, *J* = 15.6, 7.2 Hz, 2H), 3.07−3.14 (m, 2H), 3.58−3.63 (m, 2H), 6.49−6.52 (m, 2H), 6.75−6.78 (m, 2H), 7.26−7.29 (m, 4H), 7.41−7.43 (d, *J* = 8.1 Hz, 2H), 7.52−7.53 (d, *J* = 8.1 Hz, 2H). A sample of known concentration of the stable *trans* compound was irradiated at −40 °C with λ ≥ 280 nm. The UV−vis spectrum taken after the irradiation is the sum of the absorption of the stable *trans* compound and the unstable *cis* compound. After conversion of the unstable *cis* compound to stable *cis* compound, vide supra,

the ratio of both compounds and hence their concentrations were determined (HPLC, isosbestic point: 273 nm). Since both concentrations and the ϵ of the stable *trans* compound are known, the UV−vis spectrum of the unstable *cis* compound can be calculated according to $A = \epsilon_{stable\ trans} \cdot c_{stable\ trans} \cdot l + \epsilon_{unstable\ cis} \cdot c_{unstable\ cis} \cdot l$. The UV−vis spectrum of the unstable *trans* compound was obtained in a similar way. (2*R*,2′*R*)-(*M,M*)-*cis*-**3**: UV−vis (calculated, *n*-hexane) $\lambda_{max}(\epsilon)$: 221 (80 700), 264 (27 100), 305 (8800), 317 (10 400), 397 (16 900). (2*R*,2′*R*)-(*M,M*)-*trans*-**3**: UV−vis (calculated, *n*-hexane): $\lambda_{max}(\epsilon)$ 218 (95 600), 260 (27 900), 392 (23 400). The CD spectra of the unstable compounds have been calculated in a similar fashion as the UV−vis spectra. A sample of known concentration of the stable *trans* compound was irradiated at −40 °C with λ ≥ 280 nm. The CD spectrum taken after the irradiation is the sum of the CD signal of the stable *trans* compound and the unstable *cis* compound. After conversion of the unstable *cis* compound to the stable *cis* compound, vide supra, the ratio of both compounds and hence their concentrations can be determined (HPLC, isosbestic point: 273 nm). Since both concentrations and the $\Delta\epsilon$ of the stable *trans* compound are known, the CD spectrum of the unstable *cis* compound can be calculated according to $\Theta = (3.3 \times 10^5 \times \Delta\epsilon_{stable\ trans} \cdot c_{stable\ trans} \cdot l)/M + (3.3 \times 10^5 \times \Delta\epsilon_{unstable\ cis} \cdot c_{unstable\ cis} \cdot l)/M$. The CD spectrum of the unstable *trans* compound was obtained in a similar way. (2*R*,2′*R*)-(*P,P*)-*cis*-**3**: CD (*n*-hexane) λ (Δϵ): 209.4 (30.4), 214.8 (65.6), 224.6 (−28.4), 231.4 (99.5), 269.8 (−172.5), 373.0 (−7.3). (2*R*,2′*R*)-(*M,M*)-*cis*-**3**: CD (calculated, *n*-hexane) λ (Δϵ): 222.2 (133.8), 231.8 (−161.9), 251.2 (−48.5), 259.8 (−78.6), 279.2 (96.4), 343.4 (0.9), 395.8 (11.7). (2*R*,2′*R*)-(*P,P*)-*trans*-**3**: CD (*n*-hexane) λ (Δϵ): 214.0 (−156.4), 220.6 (36.0), 226.8 (−154.8), 236.6 (13.0), 248.4 (−85.7), 251.6 (−59.1), 258.0 (−236.5), 266.4 (8.5), 280.8 (−12.1), 285.8 (−8.9), 298.2 (−15.3), 330.0 (10.6), 351.8 (21.5), 366.6 (20.6). (2*R*,2′*R*)-(*M,M*)-*trans*-**3**: CD (calculated, *n*-hexane) λ (Δϵ): 215.6 (106.0), 221.2 (−18.1), 230.4 (98.6), 247.0 (−10.4), 253.4 (20.9), 258.0 (5.8), 269.2 (55.7), 297.6 (−3.9), 317.2 (−0.3), 388.4 (−24.2).

2-Methyl-2,3-dihydro-1*H*-cyclopenta[*a*]naphthalen-1-one 4. Ketone **4** was prepared in a similar fashion as that decribed below for the enantiomerically pure ketone (*R*)-**4** from acid chloride **8**. However, for the Friedel−Crafts reaction toluene was used instead of dichloroethane as the solvent.

(2*R*)-2-Methyl-2,3-dihydro-1*H*-cyclopenta[*a*]naphthalen-1-one (*R*)-4. A mixture of acid (*R*)-**5** (0.55 g, 2.6 mmol) in a solution of SOCl$_2$ (1.3 mL), DMF (2 drops), and CH$_2$Cl$_2$ (50 mL) was refluxed for 1 h. The volatiles were removed under reduced pressure, and the remaining yellow oil was dissolved in dichloroethane (100 mL) and the solution cooled to 0 °C. There was added quickly AlCl$_3$ (0.69 g, 5.2 mmol, 2 equiv), and the reaction mixture was stirred for 45 min. Quenching with a saturated aqueous solution of NaHCO$_3$ (200 mL), extraction with CH$_2$Cl$_2$ (3 × 50 mL), and drying over MgSO$_4$ gave the ketone (*R*)-**4** as a slighly yellow oil (0.44 g, 2.2 mmol, 86%). HPLC: ee = 99%. [α]$_D^{20}$ = −95.7° (*c* = 0.65, CHCl$_3$). ^{1}H NMR (300 MHz, CDCl$_3$) δ: 1.37−1.39 (d, *J* = 7.0 Hz, 3H), 2.77−2.87 (m, 2H), 3.44−3.53 (dd, *J* = 16.0, 8.1 Hz, 1H), 7.49−7.52 (d, *J* = 8.4 Hz, 1H), 7.53−7.58 (m, 1H), 7.65−7.70 (m, 1H), 7.88−7.91 (d, *J* = 8.1 Hz, 1H), 8.03−8.06 (d, *J* = 8.4 Hz, 1H), 9.14−9.17 (d, *J* = 8.4 Hz, 1H). ^{13}C NMR (75.48 MHz, CDCl$_3$) δ: 16.1 (q), 34.7 (t), 41.8 (d), 123.38 (d), 123.43 (d), 126.0 (d), 127.6 (d), 128.2 (d), 129.0 (s), 129.5 (s), 132.1 (s), 135.1 (d), 156.1 (s), 209.2 (s). *m/z* (EI, %) = 196 (M^+, 100), 181 (83). HRMS (EI): calcd. for $C_{14}H_{12}O$ 196.0888, found 196.0898. Determination of ee by HPLC using a Daicel Chiralcel OB−H column, heptane:*i*-propanol = 99:1, t_{ret}(*S*)-**4**: 19.3 min, t_{ret}(*R*)-**4**: 22.1 min.

2-Methyl-3-naphthalen-2-yl-propionic Acid 5. A mixture of ester **7** (1.72 g, 7.5 mmol), KOH (6.0 g), EtOH (30 mL), and water (30 mL) was heated at reflux overnight. Acidification of the reaction mixture with 30% HCl and extraction with Et$_2$O (3 × 100 mL), washing of the combined organic layers with water (3 × 100 mL), followed by drying over MgSO$_4$ gave after removal of the solvent the acid **5** as a white solid (1.4 g, 6.5 mmol, 87%). mp 87.4−88.4 °C.

(2*R*)-2-Methyl-3-naphthalen-2-yl-propionic Acid (*R*)-5. In a mixture of THF and water (4:1, 125 mL) was dissolved **10** (6.20 g, 16.6 mmol). To the stirred ice-cooled solution was then added dropwise at 0 °C H_2O_2 (30% aqueous solution, 7.0 mL, 70 mmol). After 5 min, a solution of LiOH (0.65 g, 27 mmol) in water (5 mL) was added slowly and the reaction mixture was subsequently stirred for 90 min. A solution of Na_2SO_3 (9.0 g, 69 mmol) in water (25 mL) was added, and stirring was continued for 45 min at room temperature. The major part of the THF was removed under reduced pressure, and the basic solution was extracted with CH_2Cl_2 (3 × 100 mL) to remove the chiral auxiliary. Acidification with 10% HCl and extraction with CH_2Cl_2 (3 × 100 mL) gave after drying over Na_2SO_4 and removal of the organic solvents the acid (*R*)-**5** as a white solid (3.24 g, 15.1 mmol, 90%), mp 82.8−83.8 °C. $[\alpha]_D^{20} = -26.1°$ ($c = 1.75$, CHCl₃). ¹H NMR (300 MHz, CDCl₃) δ: 1.21−1.24 (d, $J = 7.0$ Hz, 3H), 2.81−2.93 (m, 2H), 3.23−3.29 (m, 1H), 7.32−7.35 (dd, $J = 8.4$, 1.5 Hz, 1H), 7.42−7.50 (m, 2H), 7.65 (s, 1H), 7.77−7.84 (m, 3H); ¹³C NMR (75.48 MHz, CDCl₃): δ 16.5 (q), 39.3 (t), 41.1 (d), 125.4 (d), 126.0 (d), 127.3 (d), 127.4 (d), 127.5 (d), 127.6 (d), 128.0 (d), 132.2 (s), 133.4 (s), 136.5 (s), 182.8 (s). *m/z* (EI, %) = 214 (M^+, 58), 141 (100). HRMS (EI): calcd. for $C_{14}H_{14}O_2$ 214.0994, found 214.1010.

2-Methyl-3-naphthalen-2-yl-propionic Acid Methyl Ester 7. A LDA solution in THF (100 mL) was prepared at −50 °C by adding *n*-BuLi (10 mL, 16 mmol) to diisopropylamine (2.25 mL, 16 mmol) followed by stirring for 15 min at −50 °C. Subsequently, methyl propionate (1.53 mL, 16 mmol) was added dropwise at −60 °C and the resulting mixture was stirred for 1 h at approximately −60 °C. The bromide **6**[26] (3.9 g, 17.6 mmol) dissolved in THF (20 mL) was added slowly, and the reaction mixture was allowed to warm overnight to room temperature. Addition of a saturated aqueous solution of NH₄Cl (200 mL) and extraction with Et₂O (2 × 100 mL), drying of the organic layers (MgSO₄), and evaporation of the solvent gave a yellow oil. Purification by column chromatography (SiO₂, heptane:ethyl acetate = 16:1, $R_f = 0.4$) provided ester **7** as a colorless oil (1.75 g, 7.6 mmol, 48%).

(2*R*)-2-Methyl-3-naphthalen-2-yl-propionic Acid Methyl Ester (*R*)-7. A mixture of acid (*R*)-**5** (15 mg, 70 μmol), iodomethane (0.25 mL, 4.0 mmol), and K₂CO₃ (110 mg, 0.80 mmol) in DMF (2 mL) was stirred overnight at room temperature. After addition of ether (25 mL), the reaction mixture was washed with water (5 × 25 mL). The organic layer was dried (MgSO₄) and the solvent removed under reduced pressure to give the ester (*R*)-**7** as a colorless oil (14 mg, 61 μmol, 87%). HPLC: ee > 99%. ¹H NMR (300 MHz, CDCl₃) δ: 1.18−1.20 (d, $J = 6.2$ Hz, 3H), 2.79−2.89 (m, 2H), 3.16−3.19 (m, 1H), 3.64 (s, 3H), 7.29−7.32 (d, $J = 8.4$ Hz, 1H), 7.42−7.48 (m, 2H), 7.61 (s, 1H), 7.73−7.79 (m, 3H); ¹³C NMR (75.48 MHz, CDCl₃) δ: 16.6 (q), 39.6 (t), 41.1 (d), 51.3 (q), 125.1 (d), 125.7 (d), 127.1 (2xd), 127.3 (d), 127.4 (d), 127.8 (d), 132.0 (s), 133.3 (s), 136.6 (s), 176.1 (s). *m/z* (EI, %) = 228 (M^+, 38), 141 (100). HRMS (EI): calcd. for $C_{15}H_{16}O_2$ 228.1150,

found 228.1141. Determination of ee by HPLC using a Daicel Chiralcel OB−H column, heptane:*i*-propanol = 99:1, $t_{\text{ret}}(R)$-**7**: 23.6 min, $t_{\text{ret}}(S)$-**7**: 26.3 min.

2-Methyl-3-naphthalen-2-yl-propionyl Chloride 8. A mixture of acid **5** (0.51 g, 2.4 mmol), SOCl₂ (2.0 mL), DMF (2 drops), and CH₂Cl₂ (20 mL) was refluxed for 1 h. All volatiles were distilled off under reduced pressure, giving the acid chloride **8** as a yellow oil (0.55 g, 2.4 mmol, 98%), which was used immediately in the subsequent reaction. ¹H NMR (300 MHz, CDCl₃) δ: 1.31−1.33 (d, $J = 6.6$ Hz, 3H), 2.89−2.96 (ddd, $J = 13.6$, 6.3, 1.8 Hz, 1H), 3.23−3.39 (m, 2H), 7.30−7.33 (dd, $J = 8.4$, 1.8 Hz, 1H), 7.43−7.49 (m, 2H); 7.65 (s, 1H), 7.79−7.84 (m, 3H).

(4*S*)-4-Benzyl-3-((2*R*)-2-methyl-3-naphthalen-2-yl-propionyl)-oxazolidin-2-one 10. Freshly prepared LDA (44 mmol) in THF (150 mL) was cooled to −80 °C. A solution of **9** (8.85 g, 39.7 mmol) in THF (50 mL) was slowly added at −80 °C, and the mixture was kept at this temperature for 2 h. The temperature was then slowly raised to 0 °C, bromide **6**[26] (20 g, 90 mmol) dissolved in THF (50 mL) added, and the reaction mixture allowed to stir overnight. After quenching with a saturated aqueous solution of NH₄Cl (300 mL), the reaction mixture was extracted with Et₂O (2 × 100 mL), the combined organic layers were dried (MgSO₄), and the solvents removed under reduced pressure. The crude product was purified by flash column chromatography (SiO₂), first with a mixture of heptane:ethyl acetate = 16:1 to remove the excess bromide and then with a heptane:ethyl acetate = 8:1 mixture. The resulting colorless solid was recrystallized from a heptane:ethyl acetate mixture, giving the desired product **10** diastereomerically pure as white fluffy crystals (7.95 g, 21.3 mmol, 54%), mp 134.9−135.1 °C. $[\alpha]_D^{20}$ = +15.4° ($c = 4.05$, CHCl₃). ¹H NMR (300 MHz, CDCl₃) δ: 1.22− 1.24 (d, $J = 7.0$ Hz, 3H), 2.46−2.49 (dd, $J = 13.6$, 9.2 Hz, 1H), 2.80− 2.87 (dd, $J = 13.2$, 7.7 Hz, 1H), 3.06−3.11 (dd, $J = 13.6$, 3.3 Hz, 1H), 3.30−3.37 (dd, $J = 13.2$, 7.3 Hz, 1H), 4.06−4.28 (m, 3H), 4.64− 4.72 (m, 1H), 6.96−7.00 (m, 2H), 7.18−7.21 (m, 3H), 7.40−7.49 (m, 3H), 7.72 (s, 1H), 7.78−7.82 (m, 3H). ¹³C NMR (75.48 MHz, CDCl₃) δ: 16.6 (q), 37.5 (t), 39.4 (d), 39.9 (t), 54.9 (d), 65.7 (t), 125.3 (d), 125.8 (d), 127.1 (d), 127.4 (d), 127.5 (d), 127.6 (d), 127.7 (d), 127.8 (d), 128.6 (d), 129.1 (d), 132.1 (s), 133.3 (s), 134.9 (s), 136.6 (s), 152.9 (s), 176.3 (s). *m/z* (EI, %) = 373 (M^+, 93), 168 (93), 141 (100). HRMS (EI): calcd. for $C_{24}H_{23}NO_3$ 373.1678, found 373.1675.

Supporting Information Available: ¹H NMR and APT of all reported compounds, crystallographic information files (CIF), crystallographic details, a table to convert the labels in both X-ray structures used in the paper and the cif files, and Eyring plots for both thermal helix inversion steps. This material is available free of charge via the Internet at http://pubs.acs.org. See any current masthead page for ordering information and Web access instructions.

JA036782O

(26) Adcock, W.; Dewar, M. J. S.; Golden, R.; Zeb, M. A. *J. Am. Chem. Soc.* **1975**, *97*, 2198−2205.